Inorg. Chem. **2005**, *44*, 3890–3895

First Hydrotalcite-like Sulfonate Coordination Network Incorporating Robust Cationic Layers and Flexible Interlayer Interactions

Yufeng Liu, Jiachun Su, Weihong Li,* and Jinguang Wu

State Key Laboratory of Rare Earth Materials Chemistry and Applications, College of Chemistry and Molecular Engineering, Peking University, Beijing, 100871, People's Republic of China

Received January 28, 2005

In this paper, a novel coordination network of D,L-homocysteic acid with strontium chloride is reported. This compound exhibits an infinite microporous multilayered structure, describable as one-dimensional coordination-based microtubes cross-linking into cationic layers. Chloride anions are intercalated between layers to neutralize the charge, and the layers further pack into a three-dimensional solid via electrostatic interactions and hydrogen bonding. Thermogravimetric analysis (TGA), variable-temperature Fourier transform infrared spectroscopy (FT-IR), and powder X-ray diffraction (XRD) are presented to extensively study the structure. Results show that the compound is stable up to 326 °C. Below this temperature, the layered structure is sustained in the process of the reversible loss/gain of coordinated water, confirming that the network involves a robust coordination-based cationic layer framework but rather flexible interlayer interactions. This compound and its analogies are expected to have potential applications in anion exchange and gas storage.

Introduction

In past decades, the most active expansion of crystal engineering, which has its roots in organic solid-state photochemistry, took place in the realm of inorganic, bioinorganic, and coordination chemistry.[1] Modern inorganic crystal engineering (ICE) is a hybrid discipline of supramolecular chemistry and material science, which has implication for the rational design of functional materials.[2] Regulating the performance of materials greatly relies on the control of its structure. However, it remains a challenging prospect to tailor the chemical and/or physical properties of crystalline coordination networks through crystal design at the molecular level. Up to now, the major goal of ICE is to derive relationships between a solid's structure and its properties. There is an inherent value to building such an information reservoir of networks with various topologies and potential applications, from which a series of principles can be extracted for future structure prediction. Such deposition will significantly contribute to the theories and applications of ICE; it will also accelerate the design of new materials.

A promising method for constructing functional solid-state materials is to employ the coordination bonds between organic ligands and metal ions as the basic interaction, with the combinations of some supramolecular contacts such as hydrogen bonding, $\pi-\pi$ stacking, and weak intermolecular interactions. Over recent years, much study has been centered upon the coordination networks assembled by metal ions and polycarboxylate, polypyridines, or their derivatives,[3] while the sulfonate group (RSO_3^-) is regarded as a weakly coordinating group and has been excluded from the "good" ligands for ICE. Consequently, fewer extended solids involving RSO_3^- have been reported, and most of them use aromatic sulfonate anions as synthons.[4] Studies on nonaromatic sulfonates that attached multiligating groups are seldom involved.[5]

However, ICE does not deal with only one specific group, and the synergistic effect among different functional groups should not be neglected. It is believed that carefully designed organic ligands capable of binding metal ions at a chelating site may improve the structural control and assembly.[6] The notable effect of employing multifunctional groups in

* E-mail: Weihong_Li@pku.org.cn.

(1) Schimide, G. M. J. *Pure Appl. Chem.* **1971**, *27*, 647.
(2) Braga, D. *J. Chem. Soc., Dalton Trans.* **2000**, 3705.
(3) (a) Kou, H.-Z.; Jiang, Y.-B.; Cui, A.-L. *Cryst. Growth Des.* **2005**, *5*, 77. (b) Hilderbrand, S. A.; Lippard, S. J. *Inorg. Chem.* **2004**, *43*, 5294. (c) Hu, X.-X.; Xu, J.-Q.; Cheng, P.; Chen, X.-Y.; Cui, X.-B.; Song, J.-F.; Yang, G.-D.; Wang, T.-G. *Inorg. Chem.* **2004**, *43*, 2261. (d) Crane, J. D.; Moreton, D. J.; Rogerson, E. *Eur. J. Inorg. Chem.* **2004**, 4237. (e) Dybtsev, D. N.; Chun, H.; Kim, K. *Angew. Chem., Int. Ed.* **2004**, *43*, 5033. (f) Zheng, Y.-Q.; Lin, J.-L.; Kong, Z.-P. *Inorg. Chem.* **2004**, *43* (8), 2590. (g) Ghosh, S. K.; Bharadwaj, P. K. *Inorg. Chem.* **2004**, *43*, 2293. (h) Yan, B.; Xie, Q. Y. *J. Mol. Struct.* **2004**, *688*, 73. (i) Senegas, J.-M.; Bernardinelli, G.; Imbert, D.; Bunzli, J.-C. G.; Morgantini, P.-Y.; Weber, J.; Piguet, C. *Inorg. Chem.* **2003**, *42*, 4680.

10.1021/ic0501418 CCC: $30.25 © 2005 American Chemical Society
Published on Web 05/04/2005

generating new materials with microporous or open-framework structures has been manifested by studies of metal multifunctional anionic units, such as diphosphonates, aminophosphonates, or phosphonocarboxylates.[7] Previous studies[8] and our unpublished work have also proved that some assistant groups have significant impact on the binding capability of sulfonate group with some transition metals. Thus, studying the behaviors of such synthons in the presence of different assistant groups can positively contribute to the knowledge of ICE. Upon investigating the coordinating behaviors of the ligands with multifunctional groups, we may find some specific and effective building blocks for a certain metal ion when assembling novel structures. Another advantage of introducing multiple groups is that, with an appropriate alignment of these functional groups, hydrogen bonding can easily form between H-acceptor (for example, carboxylate) and H-donor (for example, ammonium), which can probably cross-link into a higher-dimensional and more stabilized structure.

In this work, we chose D,L-homocysteic acid, **L**, presenting three distinct ligating functional groups ($-SO_3^-$, $-COOH$, and $-NH_3^+$) attached to an alkyl chain, as the ligand in our experiments. Herein, we report the coordination framework of [Sr(**L**)(H_2O)]Cl, **1**.

Experimental Section

Materials and Methods. All the chemicals were of reagent grade and were used without further purification. Infrared spectra were recorded on a Nicolet Magana 750 II Fourier transform IR spectrometer with a NIC-Plan microscope. Elementary analyses (C, H, N) were conducted by the Analysis Center at Peking University. TGA trace was performed on a DuPont 1090B TGA 951 over the temperature range 25−400 °C at a linear heating rate of 10 °C/min.

Synthesis of [Sr(L)(H_2O)]Cl. D,L- Homocysteic acid, **L** (0.55 g, 3.0 mmol), and $SrCl_2$ (0.81 g, 3.0 mmol) were dissolved in a binary mixture solvent of H_2O/ethanol. The pH of the reaction mixture was adjusted to 4.0 by dropwise addition of NaOH (1 mol L^{-1}). The resulting solution was carefully concentrated on a water bath, and then filtered into a 25 × 40 mm glass vial, which was allowed to stand at room temperature. Colorless single crystals suitable for X-ray data collection were yielded within one week. Elemental analysis calcd (%) for [Sr($C_4H_8NO_5S$)(H_2O)]Cl: C 14.86, H 3.12, N 4.33, S 9.92; found: C 14.63, H 3.16, N 4.32, S 9.54.

A large amount of polycrystalline solid can be acquired by a similar but simpler method. After the hot concentrated solution was cooled to room temperature, adding ethanol will facilitate yielding fine colorless powder. **L** (1.211 g, 6.62 mmol) and $SrCl_2$ (1.634 g, 6.13 mmol) yielded 1.667 g of product (84.1%). Elemental analysis calcd (%): C 14.86, H 3.12, N 4.33, S 9.92; found: C 14.74, H 3.18, N 4.42, S 9.46. FT-IR and powder X-ray diffraction further demonstrated that the phase of this powder was identical to that of the single crystal.

X-ray Crystallography. Diffraction data were collected on a nonius KappaCCD diffractometer using monochromatic Mo Kα radiation (0.71073 Å) at 293 K. The final cycle of full-matrix least-squares refinement was based on 2466 observed reflections. Calculations were completed with the SHELX-97 program.[9] All nonhydrogen atoms were refined anisotropically. Hydrogen atoms of the water molecule and $-NH_3^+$ were located from Fourier difference maps, while hydrogen atoms attached to carbons were generated using a riding model. Crystal structure data for compound **1** are summarized in Table 1. Selected bond lengths and angles are given in Table 2. CCDC-247788 contains the supplementary crystallographic data for this compound. These data can be obtained free of charge via www.ccdc.cam.ac.uk/data_request/cif, by e-mailing data_request@ccdc.cam.ac.uk, or by contacting The Cambridge Crystallographic Data Centre, 12, Union Road, Cambridge CB2 1EZ, UK; fax: +44 1223 336033.

Powder X-ray diffraction data were collected on a Bruker D8 Advance X-ray diffraction meter using monochromatic Mo Kα radiation (1.54056 Å) and a 0.02° step scan from 4° to 40° in 2θ.

Table 1. Crystal Data and Structure Refinement of Compound **1**

empirical formula	[Sr($C_4H_8NO_5S$)(H_2O)]Cl
fw	323.26
cryst syst	monoclinic
space group	P2(1)/n
a (Å)	4.87070(10)
b (Å)	9.1016(2)
c (Å)	24.2355(6)
β (deg)	91.1059(11)
V (Å^3)	1074.19(4)
Z	4
D_{calcd} (g/cm^3)	1.999
abs coeff (mm^{-1})	5.465
F(000)	640
cryst size (mm^3)	0.35 ×0.25 ×0.20
reflns collected	14330
indep reflns [R(int)]	2466 [0.0681]
data/restraints/parameters	2466/3/147
GOF on F^2	1.030
final R indices [$I > 2\sigma(I)$]	$R_1 = 0.0428$, $wR_2 = 0.1107$
R Indices (all data)	$R_1 = 0.0624$, $wR_2 = 0.1193$

(4) (a) Côté, A. P.; Shimizu, G. K. H. *Inorg. Chem.* **2004**, *43*, 6663. (b) Mahmoudkhani, A. H.; Côté, A. P.; Shimizu, G. K. H. *Chem. Commun.* **2004**, 2678. (c) Kennedy, A. R.; Kirkhouse, J. B. A.; McCarney, K. M.; Puissegur, O.; Smith, W. E.; Staunton, E.; Teat, S. J.; Cherryman, J. C.; James, R. *Chem. Eur. J.* **2004**, *10*, 4606. (d) Cai, J. *Coord. Chem. Rev.* **2004**, *248*, 1061. (e) Côté, A. P.; Shimizu, G. K. H. *Coord. Chem. Rev.* **2003**, *245*, 49. (f) Côté, A. P.; Shimizu, G. K. H. *Chem. Eur. J.* **2003**, *9*, 5361. (h) Shimizu, G. K. H.; Enright, G. D.; Ratcliffe, C. I.; Rego, G. S.; Reid, J. L.; Ripmeester, J. A. *Chem. Mater.* **1998**, *10*, 3282. (i) Smith, G.; Cloutt, B. A.; Lynch, D. E.; Byriel, K. A.; Kennard, C. H. L. *Inorg. Chem.* **1998**, *37*, 3236.

(5) (a) Riley, P. J.; Reid, J. L.; Côté, A. P.; Shimizu, G. K. H. *Can. J. Chem.* **2002**, *80*, 1584. (b) Côté, A. P.; Ferguson, M. J.; Khan, K. A.; Enright, G. D.; Kulynych, A. D.; Dalrymple, S. A.; Shimizu, G. K. H. *Inorg. Chem.* **2002**, *41*, 287.

(6) Robson, R. *J. Chem. Soc., Dalton Trans.* **2000**, 3735.

(7) (a) Costantino, U.; Nocchetti, M.; Vivani, R. *J. Am. Chem. Soc.* **2002**, *124*, 8428. (b) Mao, J.-G.; Wang, Z.; Clearfield, A. *Inorg. Chem.* **2002**, *41*, 6106. (c) Galdecka, E.; Galdecki, Z.; Gawryszewska, P.; Legendziewicz, J. *New J. Chem.* **2000**, *24*, 387. (d) Zheng, L.-M.; Yin, P.; Xin, X.-Q. *Inorg. Chem.* **2002**, *41*, 4084. (e) Stock, N.; Frey, S. A.; Stucky, G. D.; Cheetham, A. K. *J. Chem. Soc., Dalton Trans.* **2000**, 4292. (f) Ayyappan, S.; Delgado, G. D.; Cheetham, A. K.; Ferey, G.; Rao, C. N. R. *J. Chem. Soc., Dalton Trans.* **1999**, 2905. (g) Fredoueil, F.; Evain, M.; Massiot, D.; Bujoli-Doeuff, M.; Janvier, P.; Clearfield, A.; Bujoli, B. *J. Chem. Soc., Dalton Trans.* **2002**, 1508. (h) Gutschke, S. O. H.; Price, D. J.; Powell, A. K.; Wood, P. T. *Angew. Chem., Int. Ed.* **1999**, *38*, 1088. (i) Vivani, R.; Costantino, U.; Nocchetti, M. *J. Mater. Chem.* **2002**, *12*, 3254.

(8) (a) Cai, J.; Chen, C.-H.; Feng, X.-L.; Liao, C.-Z.; Chen, X.-M. *J. Chem. Soc., Dalton Trans.* **2001**, 2370. (b) Chen, C.-H.; Cai, J.; Liao, C.-Z.; Feng, X.-L.; Chen, X.-M.; Ng, S.-W. *Inorg. Chem.* **2002**, *41*, 4967. (c) Cai, J.; Chen, C.-H.; Liao, C.-Z.; Yao, J.-H.; Hu, X.-P.; Chen, X.-M. *J. Chem. Soc., Dalton Trans.* **2001**, 1137. (d) Cai, J. W.; Chen, C. H.; Zhou, J. S. *Chin. J. Inorg. Chem.* **2003**, *19*, 81. (e) Yang, J.; Ma, J.-F.; Wu, D.-M.; Guo, L.-P.; Liu, J.-F. *J. Mol. Struct.* **2003**, *657*, 333. (f) Yang, J.; Ma, J.-F.; Wu, D.-M.; Guo, L.-P.; Liu, J.-F. *Transition Met. Chem.* **2003**, *28*, 788.

(9) Sheldrick, G. M. SHELX97, Program for X-ray Crystal Structure Solution and Refinement; Göttingen University, Germany, 1997.

Table 2. Selected Bond Lengths and Angles for Compound **1**[a]

bond	length (Å)	bond	length (Å)
Sr(1)−O(4)#1	2.498(4)	S(1)−O(1)	1.471(4)
Sr(1)−O(6)	2.501(4)	C(4)−O(4)	1.231(6)
Sr(1)−O(5)#2	2.544(3)	C(4)−O(5)	1.256(6)
Sr(1)−O(2)#3	2.557(4)	O(1)−Sr(1)#5	2.651(4)
Sr(1)−O(3)#4	2.582(3)	O(2)−Sr(1)#7	2.557(4)
Sr(1)−O(1)#5	2.651(4)	O(3)−Sr(1)#4	2.582(3)
Sr(1)−O(1)	2.654(4)	O(4)−Sr(1)#8	2.498(4)
S(1)−O(3)	1.448(4)	O(5)−Sr(1)#6	2.544(3)
S(1)−O(2)	1.449(4)		

bond	angles (deg)	bond	angles (deg)
O(4)#1−Sr(1)−O(6)	86.20(17)	O(5)#2−Sr(1)−O(1)	135.28(11)
O(4)#1−Sr(1)−O(5)#2	72.21(12)	O(2)#3−Sr(1)−O(1)	76.47(12)
O(6)−Sr(1)−O(5)#2	78.69(14)	O(3)#4−Sr(1)−O(1)	76.42(11)
O(4)#1−Sr(1)−O(2)#3	75.37(13)	O(1)#5−Sr(1)−O(1)	76.62(12)
O(6)−Sr(1)−O(2)#3	78.98(14)	O(3)−S(1)−O(2)	114.0(2)
O(5)#2−Sr(1)−O(2)#3	141.49(12)	O(3)−S(1)−O(1)	111.9(2)
O(4)#1−Sr(1)−O(3)#4	124.78(13)	O(2)−S(1)−O(1)	111.0(2)
O(6)−Sr(1)−O(3)#4	131.18(16)	O(4)−C(4)−O(5)	126.0(5)
O(5)#2−Sr(1)−O(3)#4	77.41(12)	O(4)−C(4)−C(3)	118.6(4)
O(2)#3−Sr(1)−O(3)#4	139.75(12)	O(5)−C(4)−C(3)	115.4(4)
O(4)#1−Sr(1)−O(1)#5	91.55(12)	S(1)−O(1)−Sr(1)#5	132.3(2)
O(6)−Sr(1)−O(1)#5	151.81(14)	S(1)−O(1)−Sr(1)	121.3(2)
O(5)#2−Sr(1)−O(1)#5	127.20(12)	Sr(1)#5−O(1)−Sr(1)	103.38(11)
O(2)#3−Sr(1)−O(1)#5	73.28(12)	S(1)−O(2)−Sr(1)#7	138.6(2)
O(3)#4−Sr(1)−O(1)#5	71.88(11)	S(1)−O(3)−Sr(1)#4	135.2(2)
O(4)#1−Sr(1)−O(1)	151.57(12)	C(4)−O(4)−Sr(1)#8	165.3(3)
O(6)−Sr(1)−O(1)	92.27(16)	C(4)−O(5)−Sr(1)#6	115.0(3)

[a] Symmetry transformations used to generate equivalent atoms: #1 $x-1,y-1,z$; #2 $x,y-1,z$; #3 $x-1,y,z$; #4 $-x+2,-y+1,-z+1$; #5 $-x+1,-y+1,-z+1$; #6 $x,y+1,z$; #7 $x+1,y,z$; #8 $x+1,y+1,z$.

Results and Discussion

X-ray Crystal Structure. Single-crystal X-ray study of compound **1** indicates the formation of a novel network assembled by infinite cationic layers in the *ab* plane and intercalated chloride anions that bridge adjacent layers. The structure of alternating cationic and anionic layers, which bears a high analogy to hydrotalcite, is first observed in the domain of sulfonate-based coordination polymers, though a solid concerning a cationic framework with Cl^--occupied channels was previously reported.[10] A unique feature of the alternating-layered network is that the void between layers may be modifiable, so that various anions of different sizes can be intercalated into the interlayer.

The aggregation pattern of the product is that each **L** acts as a hexadentate bridging spacer linking six different strontium centers, and each strontium is coordinated by seven oxygen atoms. These oxygen atoms are from four different sulfonate groups (Sr(1)−O(1), 2.651(4) Å; Sr(1)−O(1)#5, 2.654(4) Å; Sr(1)−O(2)#3, 2.557(4) Å; Sr(1)−O(3)#4, 2.582(3) Å), two different carboxylate groups (Sr(1)−O(4)#1, 2.498(4) Å; Sr(1)−O(5)#2, 2.544(3) Å), and a water molecule that projects into the interlayer (Sr(1)−O(6), 2.501(4) Å). Each sulfonate group bridges four different Sr^{2+} using all its three oxygen atoms with a coordination mode of $\eta^3\mu^4$ (Figures 1 and 2).

Considering a single layer (Figure 3), the regularly lined Sr^{2+} centers along the *a*-axis are first bridged by a series of carboxylate and sulfonate groups from different ligands which lie along the *b*-axis. A 1:1 ratio of D- and L- optical isomers of **L** are observed herein, with each species arrayed in an individual plane and bending in opposite directions (Figure 2). The other ends of these ligands connect to another line of Sr^{2+} centers, giving rise to a 1D microtube extending along the *a*-axis. These microtubes are further cross-linked by additional metal sulfonate and metal carboxylate interactions to yield layers. The channel in the center of each microtube is hydrophobic, with a dimension of approximately 5.6 × 6.6 Å. Two views of a single microtube are depicted

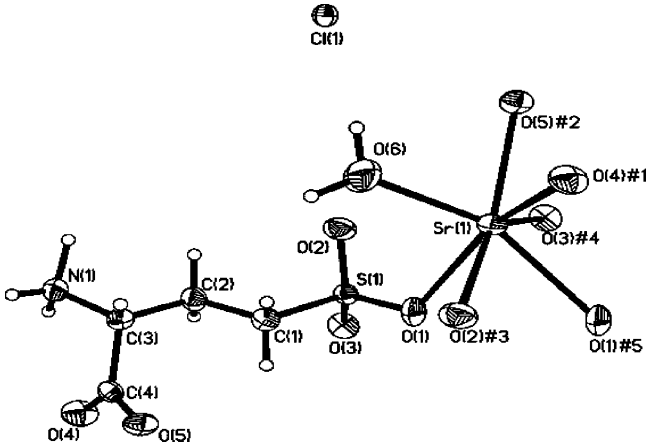

Figure 1. The structure and atom numbering scheme of $[Sr(C_4H_8NO_5S)(H_2O)]Cl$. Symmetry code: #1 $x-1,y-1,z$; #2 $x,y-1,z$; #3 $x-1,y,z$; #4 $-x+2,-y+1,-z+1$; #5 $-x+1,-y+1,-z+1$.

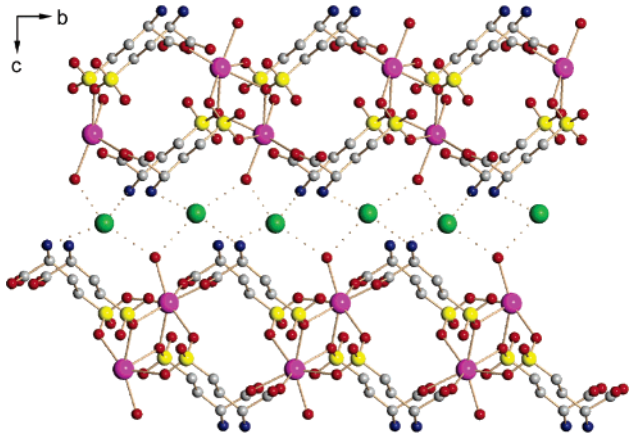

Figure 2. View a little off the *a*-axis of structure **1**, showing the layered structure, intercalated chloride anions, and interrelated hydrogen bonds. Hydrogen atoms are omitted for clarity. C, gray; O, red; N, blue; S, yellow; Cl, green; Sr, purple.

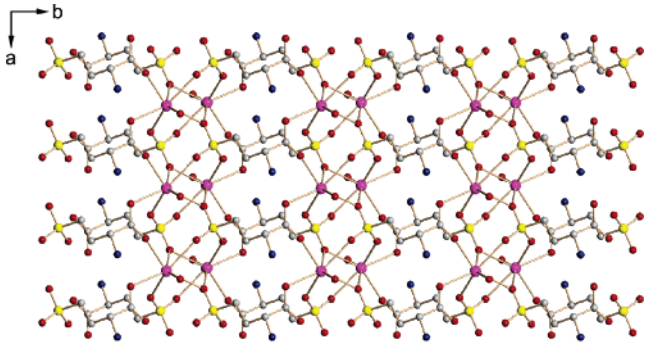

Figure 3. Top view of a single cationic layer, showing the regularly lined Sr^{2+} and the pillarlike ligand.

(10) Dalrymple, S. A.; Shimizu, G. K. H. *Chem. Eur. J.* **2002**, *8*, 3010.

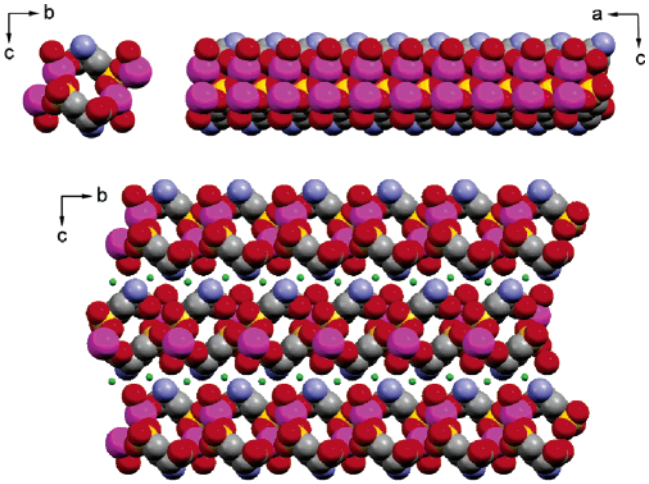

Figure 4. Space-filling views of structure **1**. Top left: cross section of a single microtube. Top right: side view of a single microtube. Bottom: Three-dimensional packing of the microtubes, clearly showing the alternating cationic and anionic layers. Chloride anions are shown as small balls for clarity.

at the top section of Figure 4. The bottom section of the same figure shows how these microtubes pack to give rise to layers and a further 3D structure.

The formation of the layered structure can be basically due to the intrinsic zwitterionic character of the preselected ligand and the multidentate feature of both sulfonate and carboxylate groups. The ligand, with $-SO_3^-$ and $-COO^-$ locating at the two opposite ends of the alkyl chain, may tend to generate a 1D chain via coordination bond where **L** acts as a columnar building block. As shown in Figure 3, it does form a barrierlike pattern with **L** serving as a pillar, but the fancy feature of "ball of Velcro"[11] makes it possible for the sulfonate group to connect with other ion centers vertically, giving the opportunity to cross-link into a higher-dimensional network.

In addition, intermolecular hydrogen bonds between the NH_3^+ and COO^- (N(1)···O(5)#2, 2.761 Å), which link these parallel ligands aligned along the *a*-axis, undoubtedly assist forming and stabilizing the supramolecular network. Furthermore, the presence of positive NH_3^+ makes the coordination-based 2D network, forming by equivalent divalent Sr^{2+} and univalent **L**, cationic. Thus, chloride anions are essential to exist among layers in order to neutralize the positive charge. The intercalation of Cl^- also causes some weak interactions, including electrostatic interactions and hydrogen bonding yielding a 3D structure. Each Cl^- forms four hydrogen bonds herein, two with $-NH_3^+$ (Cl(1)···N(1), 3.240 Å; Cl(1)···N(1A), 3.262 Å) and the other two with the coordinated water molecules (Cl(1)···O(6), 3.204 Å; Cl(1)···O(6A), 3.222 Å), orienting to the four vertexes of a distorted tetrahedron (Figure 2). As these interactions are weak and flexible, the interlayer space may be variable, giving the possibility of species exchange through the interlayer.

FT-IR and Variable-Temperature FT-IR Study. IR spectra of compound **1** and the ligand **L** were measured at room temperature, and preliminary assignments are listed in Table 3. In the spectrum of compound **1**, the presence of a sharp absorption peak at 3440 cm^{-1} (ν(O−H) of water) indicates that the water molecule exists in a stably combined state, mostly being coordinated. A series of weak peaks assigned to ν (N−H) of $-NH_3^+$ are observed in the 2800−2500 cm^{-1} region in both spectra. Although the detail of this spectral region indicates the corresponding hydrogen-bonding system rearranged, the reservation of these bands in compound **1** suggests that the amino group is protonated, and therefore it does not participate in coordination. Another apparent difference of the two spectra is in the 1800−1500 cm^{-1} spectral region, where $\nu(-COO^-)$ appears instead of ν(C═O) of −COOH. A conclusion can be drawn from the difference between $\nu_{as}(-COO^-)$ and $\nu_s(-COO^-)$ ($\Delta = 142$ cm^{-1}) that the carboxylate ion is in a bidentate bridging mode.[12] The split peaks of $\nu_{as}(-SO_3^-)$ in the spectrum of compound **1** are wider apart compared with that in **L**, and the peak of $\nu_s(-SO_3^-)$ shifts as well, indicating that the binding environment of $-SO_3^-$ varied.[13]

Table 3. IR Data of the Ligand **L** and Compound **1** (cm^{-1})

assignments	L	compound **1**
ν(O−H)		3440
ν_{as}(N−H)	3109	3099
ν_s(N−H)	2664-2553	2740-2575
$\nu_{C=O}$(−COOH)	1740	
$\nu_{as}(-COO^-)$		1581
$\nu_s(-COO^-)$		1439
$\delta_{as}(-NH_3^+)$	1595	1634
$\delta_s(-NH_3^+)$	1530	1493
$\nu_{as}(-SO_3^-)$	1207, 1179	1244, 1166
$\nu_s(-SO_3^-)$	1043	1057

Thermogravimetric analysis was measured to characterize the stability of compound **1**. A mass loss was observed from roughly 144 to 208 °C, corresponding to the loss of coordinated water molecules(5.55% obsd, 5.57% calcd). Then the compound is completely stable until the structure collapses at about 326 °C.

Variable-temperature FT-IR study (room temperature to 230 °C) was used in order to further study the stability of the compound as well as the coordination environment changes of the metal center during the process of dehydration. The resultant spectra are shown in Figure 5.

An obvious change can be observed around the ν(O−H) of H_2O accompanied with the increase of the temperature. It gradually shifts to a lower frequency with apparent intensity decrease, and it finally disappears at 220 °C. This result agrees well with that of TGA and can be attributed to the loss of the coordinated water molecules. As the band shape of ν(O−H) remains unchanged during the process, we suggest that the water molecules dismiss directly from their coordinated states whereas the rest remain in situ, and no obvious rearrangement of the hydrogen-bonding network occurs to water. Additionally, in the characteristic spectral region of N−H, minor but dramatic changes can also be

(11) Mäkinen, S. K.; Melcer, N. J.; Parvez, M.; Shimizu, G. K. H. *Chem. Eur. J.* **2001**, *7*, 5176.

(12) Nakamoto, K. *Infrared and Raman Spectra of Inorganic and Coordination Compounds*, 4th ed.; Wiley: New York, 1986.

(13) Sun, B.; Zhao, Y.; Wu, J.-G.; Yang, Q.-C.; Xu, G.-X. *J. Mol. Struct.* **1998**, *471*, 63.

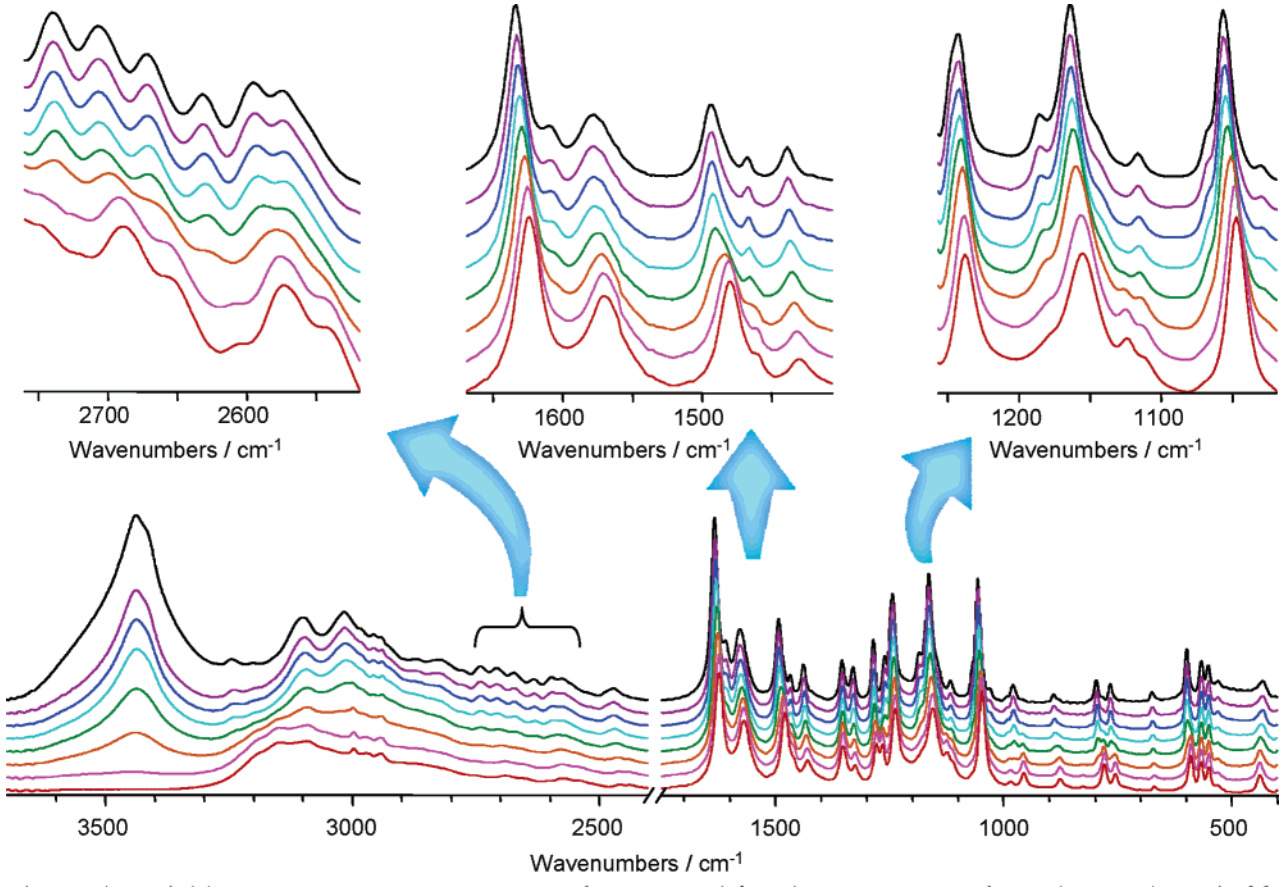

Figure 5. Variable-temperature FT-IR spectra of compound **1**. The temperature from the top down is 23, 50, 80, 110, 140, 170, 200, and 230 °C, respectively.

found, which indicates that the hydrogen-bonding network correlative with $-NH_3^+$ rearranged when losing water.

It should be noted that the characteristic stretching vibrations of both $-COO^-$ and $-SO_3^-$ shift about 10 cm^{-1} to lower frequencies after dehydration, but the difference between ν_s and ν_{as} of each group keeps approximately constant as the temperature varies. This reveals that the binding modes of $-COO^-$ and $-SO_3^-$ have no remarkable changes after the coordinated water molecules are removed.

When cooling the sample to the room temperature, most bands shift to higher frequencies. The characteristic absorption band of ν(O−H) can be observed again with a weak intensity of 0.027, suggesting that the sample can reabsorb water. To verify this consequence, the dehydrated compound was then exposed to the open air for one week and then its IR spectrum was recorded again. Result indicates that the spectrum is almost the same as that of compound **1**.

Powder X-ray Diffraction Study. The PXRD and elemental analysis of the polycrystalline sample of compound **1** match those of the single crystal, indicating the same structure (Figure 6a and 6b). To monitor the structure changes during dehydration, PXRD of the fully dehydrated sample, which was obtained by heating compound **1** up to 210 °C for an hour, was also obtained (Figure 6c).

The sharp line shapes in Figure 6c indicate that the sample is still well-crystallized after dehydration and that the network does not collapse. However, the strong (002) diffraction line exhibits noticeable shift. The calculated d_{002} value decreases

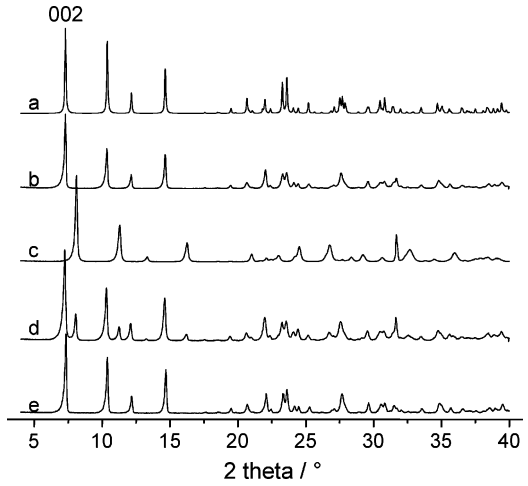

Figure 6. Powder XRD patterns of (a) simulation from the single-crystal data; (b) the polycrystalline solid sample; (c) the dehydrated sample; (d) the partly recovered sample; (e) the completely recovered sample.

from 12.11 Å (for compound **1**) to 10.90 Å (for fully dehydrated sample), indicating the interlayer distance is reduced. Interestingly, the process of losing a coordinated water molecule is reversible. The dehydrated sample can reabsorb water from the atmosphere and finally regenerate to its original phase after a long-time air exposure, and high humidity can accelerate the process. Figure 6d and 6e show the partly and fully regenerated samples, respectively. Notably, the reabsorbed water molecules not only squeeze into the interlayers and broaden the spaces to its original

value, but also reconverted to its initial coordination and hydrogen-bonding mode. This result coincides with that of variable-temperature FT-IR study. Therefore, we deduce that the network of compound **1** was sustained after removal of coordination water, and the binding modes of $-COO^-$ and $-SO_3^-$ basically remain unchanged.

The escape of water may follow two possible routes: from the channels inside the layer or from the interlayer. Considering the former one, water molecules should first break the coordination bonds and squeeze into the channel, but the steric hindrance makes such transfer mostly inaccessible. Besides, as the channel is hydrophobic, there are no appropriate binding sites in the channel that can be supplied to water. If most of the water molecules pass through the channel as unbound ones, they will undoubtedly give a corresponding band of ν(O−H) at a higher frequency than that of the coordinated ones. Unfortunately, as described above, no blue-shift of the O−H stretching band was observed in the variable-temperature FT-IR spectra. Thus, the molecules behave as if they are released to the atmosphere directly from the coordinating mode. A possible route might be described as that a water molecule transfers from one coordinating site to the adjacent one along the *a*-axis until it moves to the edge and escapes. Such transfer involves both the broken and formation of two O−H···Cl hydrogen bonds. In the completely dehydrated sample, only two N−H···Cl hydrogen bonds may survive around Cl^-. Chloride anions are more inclined to move to the vacant sites formerly occupied by water, leading to the decrease of the interlayer spaces and the reorganization of adjacent layers and hydrogen bonds. A reversed process can be figured out for the regeneration of compound **1**. This mechanism and the alterable interlayer space make it possible to exchange water for some bulky ligands, such as amines.

Conclusions

The first hydrotalcite-like sulfonate coordination network, constructing by cationic layers and interlayer chloride anions, is reported. Variable temperature FT-IR and XRD study indicated that the interlamellar bonding of compound **1** exhibits a good pliability in the heating and cooling cycle, while the cationic layer is comparatively much more stable. As hydrotalcite-like compounds have excellent performances on anion-exchange owing to their relatively weak interlayer interactions,[14] compound **1** is presumed to have the same ability. Additionally, its good performance in reversibly losing/reabsorbing the coordinated water also offers it the opportunity of intercalating other molecules such as amines instead of water.[4e] The microporous structure, analogous to a recently published work,[15] may also be a candidate as sorbent for hydrogen storage. Experiments addressing these issues are in progress.

Acknowledgment. We thank the NSF of China (2990-1002) and SRF for ROCS, SEM for financial support. We also thank Dr. Zheming Wang for collection of the single X-ray data, and Dr. Fuhui Liao for use of her PXRD.

Supporting Information Available: Crystallographic data in CIF format, additional table and figure. This material is available free of charge via the Internet at http://pubs.acs.org.

IC0501418

(14) Rives, V.; Ulibarri, M. A. *Coord. Chem. Rev.* **1999**, *181*, 61.
(15) Pan, L.; Sander, M. B.; Huang, X.; Li, J.; Smith, M.; Bittner, E.; Bockrath, B.; Johnson, J. K. *J. Am. Chem. Soc.* **2004**, *126*, 1308−1309.